Continuing investigation into possible electric fields arising from steady conduction currents*

W. F. Edwards, C. S. Kenyon, and D. K. Lemon
Utah State University, Logan, Utah 84322
(Received 10 November 1975; revised manuscript received 11 May 1976)

Recently a report was made of an effort to test higher-order, source-velocity terms in Maxwell's equations. Present electromagnetic theory predicts a zero electric field resulting from constant currents in closed conductors at rest, but Edwards has reported observing an I^2-dependent potential resulting from current I in a superconducting Nb-Ti coil. We have repeated these experiments under several variations to confirm the functional nature of the effect and to test the possibility of its arising from causes consistent with Maxwell's equations. In a fitting of the function $\phi \propto I^n$, where ϕ is the observed potential, we have obtained the value $n = 2.02 \pm 0.05$. We have also concluded that none of the following effects offers a satisfactory explanation: the self-Hall effect, configurational emf's, non-steady-current effects, thermoelectric effects, flux-flow emf's, and possible charge transfer on helium bubbles. The signal appears to be a real field effect and is as yet unexplained.

Whether or not a stationary, closed circuit carrying a constant current might produce an electric field has been a fundamental question in the history of electromagnetism. That such a field might exist occurred to physicists well over a century ago, although its size could not then be estimated. From present theoretical predictions we now know that experimental apparatus during that earlier time was not sufficiently sensitive to pick up such an effect. Nevertheless, the apparent null results of attempts to do so played a key role in the final selection by the scientific community of Maxwell's theory over those of his competitors.

In 1974 Edwards reported preliminary results of an experimental attempt to detect a second-order, current-produced, electric field.[1,2] These experiments indicated a nonzero effect. We have continued these earlier experiments testing whether or not the signal is attributable to some source consistent with the predictions of present theory. Up to this point the measurements appear to confirm the previous results.

I. HISTORICAL BACKGROUND

It has long been known that the zero- and first-order forces on a charged object near a charge-neutral, current-carrying conductor at rest in the laboratory are zero in magnitude. Throughout the history of electromagnetism all of the major theorists assumed that the *second-order* fields were also zero. This profoundly influenced the development of electromagnetic theory.

The first complete electron theory was Weber's (1848).[3,4] It encompassed the laws of Coulomb, Ampere, and Faraday, explaining all of these effects in terms of the relative motion of charged particles. Riemann's theory (1861) was also relativistic and provided an experimentally equivalent alternative to Weber's. These theories, however, predicted that conduction currents would produce an electric field unless, as was suggested by Fechner, current elements consist of equal amounts of positive and negative charge moving in opposite directions.[5,6]

Such electric fields would be dependent upon $dq\, v^2/c^2$ and other similar terms, where dq is a charge drifting with velocity $\vec{v}$. Although the quantity dqv $(=Idl)$ could be measured at that earlier time, $dq\, v^2$ could not. Maxwell wrote: "We are unable to determine whether the 'velocity of electricity' in the wire is great or small."[7] Using the Hall effect, von Ettingshausen made the first measurements of the drift speed of conduction charges in gold which, in 1880, he reported to be of the order of 1 mm/sec.[8] It is now known that $v^2/c^2 < 10^{-20}$ for essentially all cases using metallic conductors at room temperature.

The earlier physicists could not have been aware that the magnitudes of the second-order electric fields were not within the reach of the instruments of the day. In spite of this fact they appeared to be unanimously of the opinion that the fields were zero. So completely was the possible existence of such fields ruled out that Whittaker said Fechner's view of current was "almost inevitable" in the relativistic theories such as Weber's.[9]

Maxwell based his theory (1861–1873) on the field ideas of Biot, Savart, and Faraday. By adopting frame-related quantities he avoided the electric field problem of the earlier theories. Clausius developed a related electron theory (1877) stating as an "experimental assumption" that a "closed current in a stationary conductor exerts no force on stationary electricity."[10]

In the latter part of the century the view that current consisted of moving charge of only one sign began to prevail. Accompanying this was the increasing acceptance of Maxwell's theory over those of his competitors. In his history Whittaker emphasizes the close connection between the choice of a theory of current and the choice of an electromagnetic force law.[11] The link between the two was, of course, the issue concerning the current-produced electric fields.

In the controversy over the theories, the Michelson-Morley-type experiments were cited as evidence against Maxwell and the zero electric fields were cited against the relativists. By the end of the century Hertz had demonstrated electromagnetic radiation as predicted by Maxwell's theory and shortly thereafter Einstein provided the key for making Maxwell's theory relativistic.

Although the assumption that the theories must predict zero current-produced electric fields was experimentally unfounded, concern over that fact, which was never very great, diminished as Maxwell's theory gained support. Only occasionally was caution expressed, as it was by Klein in 1932:

"Hitherto it has been almost a principle of faith with physicists that an electric current exerts no force on stationary charges. But it must be admitted that as yet there are no measurements in this direction, and perhaps they cannot be made owing to the extraordinary smallness of the effect."[12]

Today, techniques for making direct measurements of the second-order electric fields are available. For this reason, the matter can finally be placed on an experimental basis.

II. PREDICTION OF MAXWELL'S THEORY

The electric field, $\vec{E}$, resulting from charges and currents is given by

$$\vec{E} = -\vec{\nabla}\phi - \frac{\partial \vec{A}}{\partial t}, \tag{1}$$

where ϕ and $\vec{A}$ are the usual retarded potentials

$$\phi(\vec{r}_2, t) = \frac{1}{4\pi\epsilon_0}\int \frac{\rho(\vec{r}_1, t')}{r}\,\delta(t' - t + r/c)\,d^3x_1\,dt', \tag{2}$$

$$\vec{A}(\vec{r}_2, t) = \frac{\mu_0}{4\pi}\int \frac{\vec{j}(\vec{r}_1, t')}{r}\,\delta(t' - t + r/c)\,d^3x_1\,dt', \tag{3}$$

where $\vec{r}_2$ and $\vec{r}_1$ are the position vectors to the field point and source point, respectively, and $\vec{r} = \vec{r}_2 - \vec{r}_1$. In a charge-neutral circuit $\rho = 0$ so ϕ is also zero. As Baker has shown, in a stationary circuit if the currents are constant $\vec{A}$ is also independent of the time so that $\partial\vec{A}/\partial t = 0$ and therefore $\vec{E} = 0$.[13]

The adoption of the point of view of an electron theory permits a comparison of Maxwell's theory with the Weber-type theories. In such an electron theory the Lienard-Wiechert potentials expressing the field of a moving charged particle in terms of retarded quantities may be obtained from (2) and (3). Using the Taylor series these then may be expanded in terms of either retarded or present quantities. To order $1/c^2$, expressed in terms of present quantities, the electric field for a charged particle is

$$\vec{E} = \int \frac{dq}{4\pi\epsilon_0}\left[\frac{\vec{n}}{r^2} + \frac{1}{2}\frac{v_1^2\vec{n}}{r^2c^2} - \frac{3}{2}\frac{(\vec{n}\cdot\vec{v}_1)^2\vec{n}}{r^2c^2} - \frac{\vec{a}_1}{2rc^2} - \frac{(\vec{n}\cdot\vec{a}_1)\vec{n}}{2rc^2}\right], \tag{4}$$

where $\rho d^3x_1 = dq$, $\vec{j}d^3x_1 = dq\,\vec{v}_1$, and the integral is over all source charges. We have introduced a somewhat subtle change in notation. Hereafter $\vec{r}$ denotes the position vector from the *moving* source particle to the field point. The quantities $\vec{v}_1$ and $\vec{a}_1$ are the velocity and acceleration, respectively, of the moving particle.

From Eq. (4) we can again confirm the fact that $\vec{E} = 0$ for constant conduction currents in closed circuits. For steady currents the distribution of moving charges along the wire is uniform. Under these conditions the integration around a closed path in Eq. (4) gives $\vec{E} = 0$. This can be seen by forming two perfect differentials

$$d_1\left(\frac{\vec{v}_1}{r}\right) = \left[\frac{\vec{a}_1}{r} + \frac{\vec{v}_1(\vec{n}\cdot\vec{v}_1)}{r^2}\right]dt \tag{5}$$

and

$$d_1\left[\frac{(\vec{n}\cdot\vec{v}_1)\vec{n}}{r}\right] = \left[\frac{(\vec{n}\cdot\vec{a}_1)\vec{n}}{r} + \frac{3(\vec{n}\cdot\vec{v}_1)^2\vec{n}}{r^2} - \frac{(\vec{n}\cdot\vec{v}_1)\vec{v}_1}{r^2} - \frac{v_1^2\vec{n}}{r^2}\right]dt. \tag{6}$$

The differential operator d_1 varies the source-point quantities, so $d_1\vec{r} = -\vec{v}_1 dt$. Since the integral around any closed path of a perfect differential is zero, the quantity

$$\frac{-I}{8\pi\epsilon_0 c^2}\,d_1\left[\frac{(\vec{n}\cdot\vec{v}_1)\vec{n}}{r} + \frac{\vec{v}_1}{r}\right] = \frac{dq}{4\pi\epsilon_0 c^2}\left[\frac{v_1^2\vec{n}}{2r^2} - \frac{3(\vec{n}\cdot\vec{v}_1)\vec{n}}{2r^2} - \frac{\vec{a}_1}{2r} - \frac{(\vec{n}\cdot\vec{a}_1)\vec{n}}{2r}\right] \tag{7}$$

integrates to zero under the conditions stated. By comparing this with Eq. (4) we see that if the conductor is charge neutral so that the Coulomb term is zero, then $\vec{E} = 0$.

III. A TEST OF MAXWELL'S THEORY

To test Maxwell's theory and the conservation of charge under the circumstances mentioned we may look for an electric field using apparatus having sufficient sensitivity to detect terms of the order of

$$\frac{1}{4\pi\epsilon_0}\int\frac{\rho v_1{}^2\vec{n}}{r^2c^2}d^3x_1\,.$$

A null measurement would confirm the theory to the same order.

A general expression for the electric field to order $1/c^2$ might contain the five terms

$$\frac{\vec{a}_1}{r},\ \frac{(\vec{n}\cdot\vec{a}_1)\vec{n}}{r},\ \frac{v_1{}^2\vec{n}}{r^2},\ \frac{(\vec{n}\cdot\vec{v}_1)^2\vec{n}}{r^2},\ \text{and}\ \frac{(\vec{n}\cdot\vec{v}_1)\vec{v}_1}{r^2}.$$

In a closed circuit these terms are not independent. If the current is constant, Eqs. (5) and (6) can be used to eliminate two of the five terms in favor of the other three. For convenience we choose to represent the field[14] as

$$\vec{E}=\frac{1}{4\pi\epsilon_0}\int\rho\left[\gamma_1\frac{v_1{}^2\vec{n}}{r^2c^2}+\gamma_2\frac{(\vec{n}\cdot\vec{v}_1)^2\vec{n}}{r^2c^2}+\gamma_3\frac{(\vec{n}\cdot\vec{v}_1)\vec{v}_1}{r^2c^2}\right]d^3x_1\,, \tag{8}$$

where the conduction charge density, ρ, is assumed to be constant. By adjusting the parameters γ_1, γ_2, and γ_3 Eq. (8) can be made to represent the $1/c^2$ electric field terms in Maxwell's theory $(\gamma_1=\gamma_2=\gamma_3=0)$. It can also represent a departure from Maxwell's theory represented by coefficients of the five terms mentioned different from those found in Eq. (4).

Of course, if a second-order, current-produced electric field does exist it may not be compatible with Eq. (8) but could have some other functional form. However, since the purpose of our experiment is to test the validity of the $1/c^2$ source terms in Maxwell's theory we must at least be able to detect an effect such as would arise were the coefficients of the terms different from zero.

The possible consequences of such a departure will not be discussed here except to note that the form of Eq. (8) with nonzero γ's would also accommodate the possibility that Maxwell's theory is correct but the charge of a moving particle is not conserved. In our experiments, a departure from Maxwell's theory is indistinguishable from a motion-dependent nonconservation of charge.

In the present experiment the field is indirectly sought by looking for a current-correlated voltage, ϕ, produced between a conducting circuit and ground. The ground consists of a conducting shield enclosing the circuit. If the current were to produce an electric field, an apparent charge, $Q=\epsilon_0\int\vec{E}\cdot d\vec{S}$, would appear on the coil so the voltage would be

$$\phi=\frac{\epsilon_0}{C}\int\vec{E}\cdot d\vec{S}\,, \tag{9}$$

where C is the circuit-to-ground capacitance of the system and the integral is over field points.

The drift velocity is given by

$$\vec{v}_1=\vec{j}/\rho\,, \tag{10}$$

where $\vec{j}$ is the current density. In general, $\vec{j}$ may vary across the cross section of a wire as well as along the length. Let $d^3x_1=dA\,dl$. If the current density is uniform over the wire cross section and if the radius of the wire is small, then $d^3x_1=Adl$, where A is the cross-sectional area. On the other hand, if the current density is not uniform, then, for a given wire element and a given field point, the field is increased by a factor α, where

$$\alpha=\frac{A}{I^2}\int j^2dA\,. \tag{11}$$

For a particular geometry the electric potential can be calculated by integrating Eq. (8) over source points and Eq. (9) over field points, resulting in

$$\phi=\frac{\kappa\alpha L}{\rho CAc^2}I^2\,. \tag{12}$$

The parameter κ is a factor which depends upon $\gamma_1,\gamma_2,\gamma_3$ and the geometry of the system. In the case of Maxwell's theory $\kappa=0$ because $\gamma_1=\gamma_2=\gamma_3=0$. For values of the γ's on the order of unity we would expect $\kappa\sim1$. For example, if $\gamma_1=1$ and $\gamma_2=\gamma_3=0$, then the electric field appears formally as a Coulomb field except for the factor v^2/c^2. In this case $dQ=\rho v^2dA\,dl/c^2$. Then if j is constant over the length of the wire, Q equals $\alpha v^2\rho AL/c^2=\alpha LI^2/\rho Ac^2$, and we find that $\kappa=1$.

A. The experimental design

The present experiments are a continuation of those reported by Edwards[1,2] which will be referred to as the *former* or *earlier* experiments.

The basic experimental design consists of a superconducting coil carrying a steady or quasi-steady current. A schematic diagram of the apparatus is shown in Fig. 1 while Fig. 2 shows a drawing of the apparatus. The potential between the coil and ground is determined for different values of the current. The electrostatic shield and all circuit elements within it are immersed in liquid helium.

The wire used for the superconducting circuit has a 48% niobium–52% titanium core of 2.5 mil

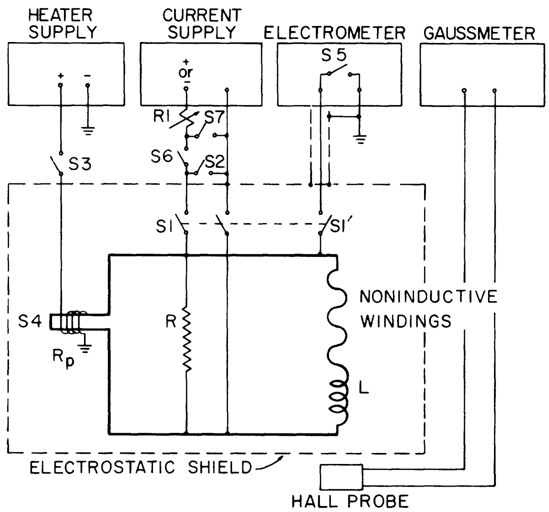

FIG. 1. Schematic diagram of the original apparatus. Details concerning the noninductive coil and the values of R and L are given in the text. The electrostatic shield and those portions of the circuit within it are immersed in liquid helium.

radius and was operated in the magnetic-field region characteristic of type-II superconductors. A copper jacket of 0.75 mil thickness surrounds the core, followed by Formvar insulation. The manufacturer reported to us that a short sample of the wire sustained 128 A giving an average core current density of 1.0×10^6 A/cm^2. He lists the critical temperature and critical field, H_{C2}, as ~10°K and 122 kG, respectively.

In order to minimize magnetic-field effects and to permit the superconductor to sustain high current densities the coil was wound using bifilar pairs except for a small number of single-wire loops to permit current monitoring through the resulting magnetic field. Both sections of the coil contributed significantly to the inductance L.

The coil consists of 701 m of wire wound in 1496 bifilar turns (2 current-opposing loops per turn). There were 19 single-wire turns in the earlier experiment and 4 in the present experiments. The nominal coil radius is 3.7 cm.

The wire has a cross section area $A = 1.3 \times 10^{-4}$ cm^2. The conduction electron density in the superconducting state was estimated to be 5.6×10^{22}/cm^3 giving $\rho = 9.0 \times 10^3$ C/cm^3.

The shield which is at ground potential consists of a brass toroidal shell surrounding the coil proper and a 6.90-cm × 6.45-cm × 5.45-cm box surrounding the shunt resistor, R, switches, and a superconducting joint. The shell and box are both of thickness $\frac{1}{32}$ in. The shield is made of thin brass, which is sufficiently resistive at liquid helium temperature to cause eddy currents, produced when the coil current is changed, to decay away in a time short compared with the time taken to change the coil current.

In the earlier experiment and in some variations of the present ones a persistent or heat switch ($S4$) appeared in the circuit. The original design described in Ref. 1 was changed in order to eliminate electrostatic induction effects. For the present experiments an 8-cm portion of the superconducting wire was bent into a double-hairpin shape and inserted into a thin cylindrical Teflon tube of radius $\frac{1}{16}$ in. containing conducting epoxy. The Teflon maintains the high coil-to-ground resistance (>10^{13} Ω). This unit was then wrapped in a heater blanket which was made of 3-mil-diameter, Teflon-insulated Constantan wire laid between 1-mil-thick, brass-foil sheets which were grounded. The heater wire was also grounded through a center tap. This shielding arrangement eliminated electrostatic induction effects. The resistance of the heater wire is approximately 30 Ω. With the system immersed in liquid helium a current of approximately 45 mA provides enough heat to keep the hairpin section of the superconductor normal. In this condition the switch has a resistance of approximately 1.4 mΩ. The leads to the heater are 5-mil-diameter Constantan wires. Later, more will be said about the heater.

With the heater on, the shunt resistor R provides the current path and forms an LR circuit. The time constant of the circuit, τ_I, is on the order of seconds which allows sufficient time to make the voltage measurements and to satisfy the condition that the current in the coil be in a quasi-steady state. The resistor is made of brass and has a resistance in the μΩ region. In most variations it has dimensions 13 mm × 14 mm × 0.8 mm and was bare, thus its surface was exposed to liquid helium. The measured values of R are given later.

The measured coil-to-ground resistance is greater than 10^{13} Ω.

The current supply is a 12-V lead acid battery. A predetermined current I_0 is established by adjusting R_I while $S7$ is closed.

The vibrating reed electrometer is a Cary model 35 having an input resistance >10^{16} Ω and an input capacitance of 50 pF. It has an available sensitivity of at least 0.15 mV. With $S1$ open and $S1'$ closed the measured circuit capacitance which includes the electrometer input capacitance is 96 pF. Switch $S1'$ appears in series with the input in order to protect the instrument from current surges in the event of failure of some portion of the circuit while the battery potential is being applied. In experimental variation II this switch

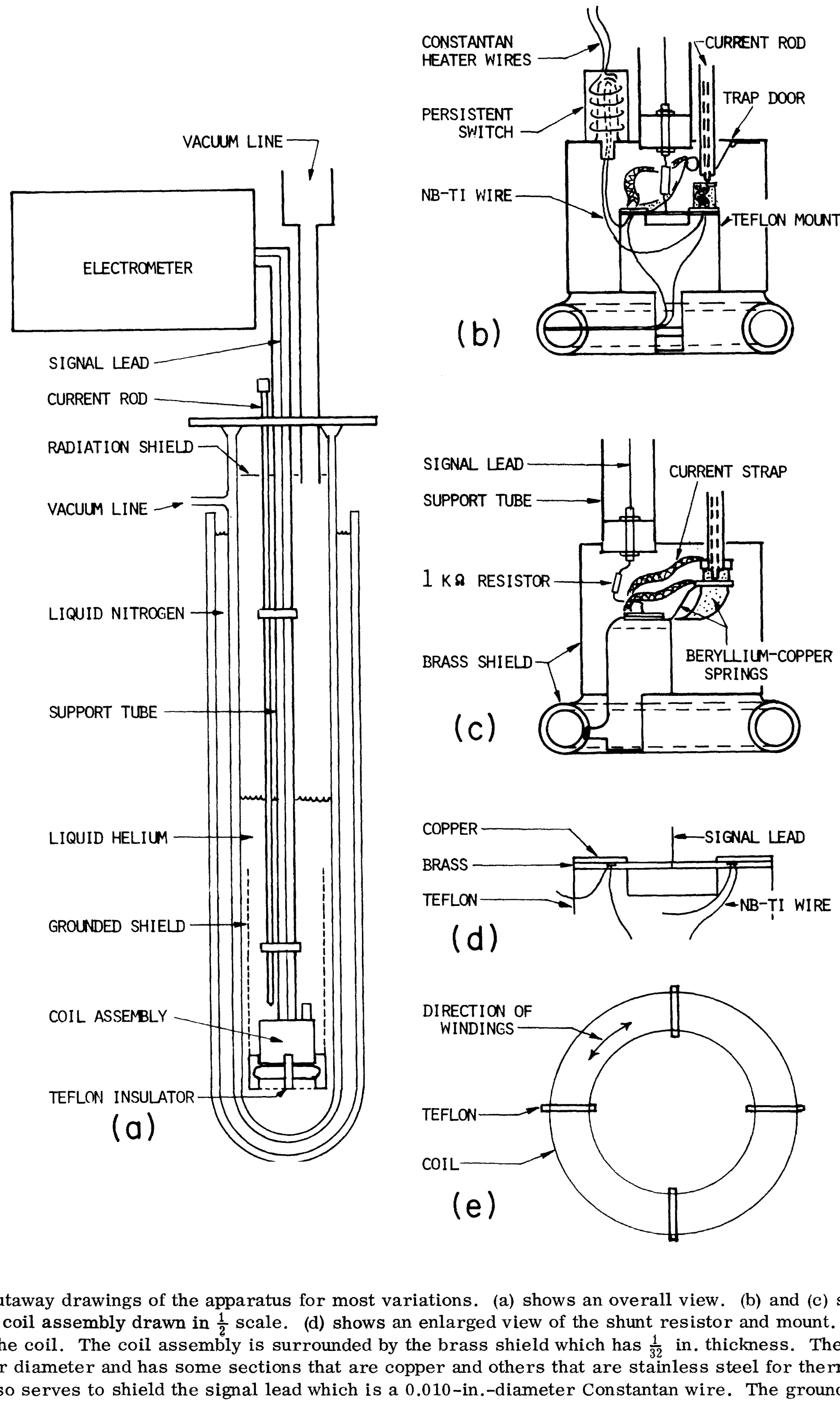

FIG. 2. Cutaway drawings of the apparatus for most variations. (a) shows an overall view. (b) and (c) show two side views of the coil assembly drawn in $\frac{1}{2}$ scale. (d) shows an enlarged view of the shunt resistor and mount. (e) shows a top view of the coil. The coil assembly is surrounded by the brass shield which has $\frac{1}{32}$ in. thickness. The support tube is $\frac{3}{4}$ in. outer diameter and has some sections that are copper and others that are stainless steel for thermal isolation. This tube also serves to shield the signal lead which is a 0.010-in.-diameter Constantan wire. The grounded shield shown in (a) was used only in variation II. The support tube was electrically grounded. The coil assembly shield was electrically insulated from the support tube and was connected to the feedback terminal of the electrometer except in variation II when it was connected to the electrometer input.

was absent and in variations III and IV it was replaced by a 1.0 kΩ resistor. Tests showed that the electrometer is insensitive to the small magnetic field produced by current in the coil.

The current is monitored using a Bell model 120 gaussmeter with a Hall-effect probe mounted outside the low-temperature Dewar flasks approximately 9.6 cm from the center of the coil and in the same plane.

Using the experimental parameters mentioned above the expected voltage, from Eq. (12), is

$$\phi = -(6.9\times 10^{-7}\ \mathrm{V/A^2}) I^2 \kappa\alpha\,. \qquad (13)$$

If κ is positive, the sign of the Coulomb-type term $v^2\vec{n}/r^2c^2$ prevails and the electric potential on the coil will bear the sign of the charge carriers.

In a superconductor the current density is not uniform across a cross section of the wire. Since α measures the amount by which the current is carried by a smaller effective cross section we expect $\alpha > 1$, resulting in a larger signal for the same current I, as seen from Eq. (13).

In addition to this, however, in a type-II superconductor the current density distribution is not expected to be unique but may vary. Experimentalists have had great difficulty detecting such changes directly since they do not affect the total current. There is, however, indirect evidence.

Bardeen and Stephen explain that transport current flows around a pinned fluxoid.[15] A high fluxoid density reduces the available superconducting cross section, thereby increasing α. Motion of pinned flux, with consequent changes in the fluxoid density, can be induced by thermal disturbances,[16,17] mechanical disturbances,[18] and by the transport current itself when near the critical state.[19]

The current-carrying properties of type-II superconductors also depends upon the history of the sample, the polarity of the current, the rate of change of the transport current, and the rate of change of any external magnetic field.[20,21] When the current is removed from a sample some flux remains pinned. Changing the direction of the current introduces fluxoids with opposite direction, some of which annihilate with the residual flux.[22] This annihilation produces heat which may induce further flux motion. A catastrophic change occurs of course when the superconductor becomes a normal conductor.

With all of these effects contributing to the fluxoid pattern it is not surprising to find α changing. In order for the results of a particular run to be unambiguous, the fluxoid pattern must remain reasonably constant due to pinning.

In our experience the α factor is observed to vary no more than about 20% for several runs. It may then jump to a value as much as a factor of 2 higher or lower; this is more probable when the current magnitude is changed by a large amount and, especially, when the coil is driven normal. After warming the coil to room temperature and cooling it again, α may return to the same range but it has been observed to return to a value differing by as much as a factor of five.

B. Procedure for making a run

A run is made as follows:

Initially $S1'$, $S2$, $S3$, $S6$, and $S7$ are open. Switches $S1$ and $S5$ are closed. The desired maximum current is established by adjusting R_I with $S7$ closed. Switch $S7$ is then opened and $S3$ is closed, which opens the persistent switch $S4$. Then $S6$ is closed and current I builds up exponentially in the circuit with the characteristic time constant $\tau_I = L/R$. The current is monitored on the gaussmeter. After I reaches the desired value, $S3$ is opened, closing $S4$. Then $S6$ is opened and because of energy stored in L the current transfers from the external source to the persistent superconducting path. To establish the high-impedance isolation of the superconducting circuit, $S1$ is opened and $S1'$, which is ganged to $S1$, and $S2$ are closed.

At this point $S5$ is opened. The electrometer now measures the potential of the coil. The base line has been shifted by grounding the circuit when the current is maximum so the expected potential becomes

$$\phi = -(6.9\times 10^{-7}\ \mathrm{V/A^2})\kappa\alpha[I(t)^2 - I_0^{\,2}]\,. \qquad (14)$$

When $S3$ is again closed, applying heat to $S4$, the current decays. Equation (14) then becomes

$$\phi = (6.9\times 10^{-7}\ \mathrm{V/A^2})\kappa\alpha I_0^{\,2}(1 - e^{-2t/\tau_I})\,, \qquad (15)$$

where $\tau_I = L/R$.

Two strong tests of any potential that appears result from the I^2 dependence of the voltage. The time constant τ_ϕ of the voltage decay should be $\frac{1}{2}$ that of the current and the potential ϕ should be independent of the direction of the current.

The magnitude of the signal constitutes another important test. From considerations of theories other than Maxwell's, if κ is not zero we may expect it to lie in the approximate range $-2 < \kappa < 2$. The parameter κ would, of course depend upon both the force law and the particular geometry. If we assume that $\kappa \sim 1$, then the limitation $\alpha \geqslant 1$ gives a minimum value for ϕ_{max} from Eq. (15). Other tests will be mentioned later.

C. Results from the previous experiment

In the earlier experiment the coil had 1496 bifilar and 19 single-wire turns resulting in an inductance 860 μH. The resistance R was 82 $\mu\Omega$ as inferred from the measured mean current decay time. The number of inductive turns and the resistance were incorrectly reported earlier as 23 and 60 $\mu\Omega$. Figure 3 shows two of the nine runs observed and one $I=0$ run. In Fig. 3 a constant potential that appeared when $S3$ was closed regardless of the condition of I can be seen. At that time it was surmised that this potential was due to improper shielding in the heat switch, therefore this baseline was subtracted from the signal.

The results from all the runs were consistent with the three tests mentioned: First, the voltage was independent of the direction of the current.

Second, the decay time for voltage was $\frac{1}{2}$ that for current. A subsequent computer analysis gave a mean decay time for the current, τ_I, of 10.4 ± 0.1 sec.[23] The mean decay time for the voltage, τ_ϕ, is 5.5 ± 0.3 sec. Calculating the exponent in $\phi\propto I^n$ for each run and finding the mean with each run weighted equally we have $n=1.93\pm0.13$ sec.

The signal magnitudes varied between 3 and 13 mV. The values of $\kappa\alpha$ ranged from 12 to 100.

It was reported that the self-Hall-effect, configurational emf's, and some terms resulting from nonsteady currents cannot explain the earlier results. We have tested each of these claims in much greater detail. Additional possibilities have been considered, including thermoelectric effects and flux motion emf's. In addition, the functional nature of the signal has been more carefully examined and some earlier experimental difficulties have been eliminated.

Following a description of the experimental variations the functional nature of the effect will be discussed. After this, each possible explanation of the effect will be thoroughly considered in the light of all of the experimental results.

IV. EXPERIMENTAL VARIATIONS

Four variations of the original experiment have been studied. Simplified schematics are shown in Fig. 4. In the first variation the number of single-wire loops in the coil was reduced. All effects dependent upon temperature, power loss in the shunt resistor, magnetic field, or stored energy would be expected to reduce. This particularly tests thermoelectric effects.

The second variation eliminated direct contacts between the coil and the electrometer and inserted a Faraday cage surrounding the coil. The potential was measured between the cage and ground. This tested the Hall effect, configurational emf's, thermoelectric emf's, flux motion emf's, contact po-

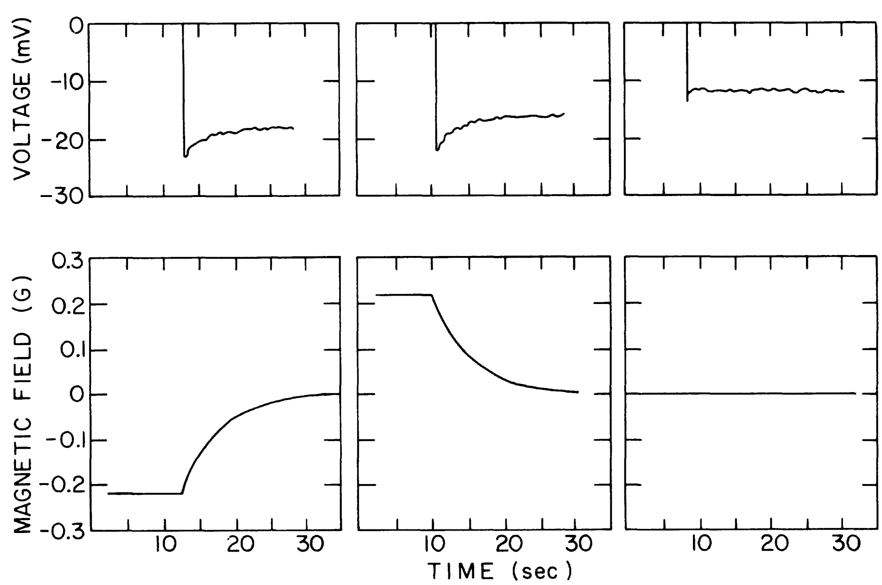

FIG. 3. Results of three experimental runs from the original experiment showing decay of the current from the persistent circuit as inferred from its magnetic field, and the corresponding voltage measured on the electrometer. The magnitude of the heater-induced voltage from run to run but the shape of the function was repeatable. This baseline was eliminated in the present experimental variations.

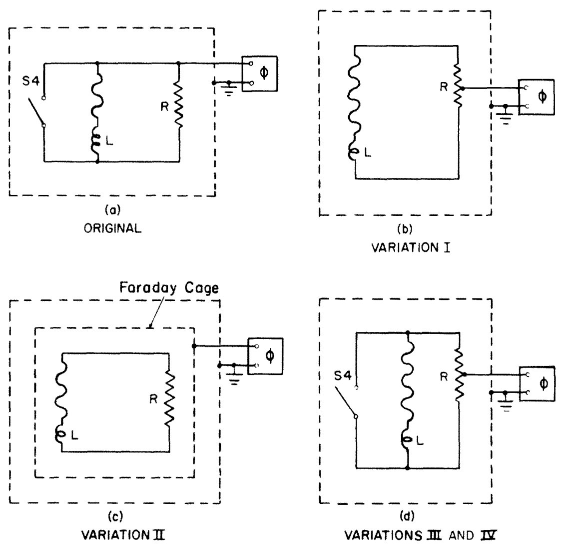

FIG. 4. Simplified circuit diagrams of the five experiments. (a) refers to the original experiment, (b) and (c) to variations I and II, respectively, and (d) to variations III and IV.

tential effects, and any effect which would redistribute the charges in the circuit leaving the total charge constant.

In the third variation a carefully shielded heat switch was used and shunt resistance R was lowered. The current decay was interrupted by alternately making the circuit persistent and decaying in order to test the functional dependence $\phi(I)$. The lowered stored energy also permitted further testing of thermoelectric effects.

A fourth variation utilized the same circuit diagram as in variation III but with the temperature of the helium lowered below the λ point in order to take advantage of the vastly improved heat transfer properties of helium II. This permitted testing the possibility of a transfer of charge on helium bubbles as well as other heat correlated effects.

A. Variation I

In this variation the number of single-wire turns was changed from 19 to 4, reducing the inductance of the coil from 860 μH to 790 μH. Otherwise the same coil was used as in the earlier experiment. To maintain a decay constant on the order of ten seconds, shunt resistance R was lowered. The measured mean decay time of the current was 6.7 sec. From τ_I and L we infer that $R = 118$ $\mu\Omega$. The capacitance to ground was ~100 pF and the stray resistance to ground was $>10^{14}$ Ω.

The signal lead was attached to the center of R rather than to one end to avoid a resulting IR potential.

As shown in Fig. 4(b) the persistent switch $S4$ was removed. This was done, first, to determine whether or not the observed effect was triggered by the application of the heat necessary to raise the temperature of the 8-cm section of superconductor from 4 °K to above the critical temperature, 10 °K, and, second, to test whether or not the constant baseline signal in the earlier experiment was indeed associated with the heater and, if so, to eliminate that potential.

Because $S4$ was eliminated the circuit never could become persistent, therefore, the procedure described earlier for making a run was modified. With $S1$, $S5$, and $S6$ closed and $S2$ and $S7$ open, current builds up in the circuit. When I reaches the desired value, as determined by the $\vec{B}$ field monitor, $S6$ is opened. The current in the superconducting circuit then immediately begins to decay through R. In a rapid sequence, $S1$ is opened, $S1'$ closed, $S2$ closed, and $S5$ opened, whereupon the electrometer begins to measure ϕ. The time lapse from the opening of $S6$ to the beginning of the measurement of ϕ was between 2 and 3 sec.

The voltage was clearly independent of the direction of the current. For five runs the mean decay times were $\tau_I = 6.7 \pm 0.2$ sec and $\tau_\phi = 2.6 \pm 0.4$ sec. The mean power-law exponent in $\phi \propto I^n$ was 2.70 ± 0.26.

The magnitudes of the voltages observed were very large considering the currents necessary to produce them. This is reflected in the size of $\kappa\alpha$, which varied from run to run between 60 and 890.

There was no detectable baseline voltage, thus confirming the conclusion that the baseline on the earlier experiment was caused by the persistent switch $S4$. The presence of the I^2 signal in the absence of a heater in $S4$ eliminates the possibility of a causal relationship between the two.

The conclusions regarding thermoelectric voltages will be discussed later.

B. Variation II

In this experiment a Faraday cage surrounded the current-bearing circuit, as shown in Fig. 4(c). The voltage between the cage and a grounded shield was measured.

The brass box and toroidal shield shown in Fig. 2 form the Faraday cage and were isolated from the superconducting circuit by Teflon insulators. A grounded shield in the shape of a cylindrical box, the sides of which were made of 18-gauge bronze screen and the bottom was made of 0.010-in.-thick beryllium-copper sheet, was inserted at the position shown. This screen was closed except at the top. Tests showed it provided sufficient shielding of the apparatus from electrostatic induction effects from charged objects in the near environment. The circuit-to-cage resistance was $>10^{14}\ \Omega$, as was the cage-to-ground resistance.

The resistance R was changed in order to increase the time constant while using the same coil as in variation I. The value of R inferred from τ_I is 64 $\mu\Omega$.

Switch $S1'$ was eliminated and switch $S1$ was modified to permit a retraction of the current leads from inside the Faraday cage. A normally closed, spring-operated trap door in the Faraday cage provided an access for the current leads.

Because of the difficulty in introducing heat through both the ground shield and the Faraday cage without introducing error signals the persistent switch $S4$ was left out of the circuit. As a result the current could not be placed in the persistent mode.

To make a run, first, with $S6$ closed, the current rod was lowered through the trap door, closing $S1$. After the current built up to an acceptable value $S1$ was opened by extracting the rod. The current, of course, immediately began decaying. Then, in rapid succession, $S6$ was opened and $S2$ closed, which grounded the rod. Then $S5$ was opened and potential measurements began. The time lapse from the opening of $S1$ to the start of electrometer measurements was between 1 and 2 sec.

Because of the movement involved in retracting the $S1$ rod, stress electric emf's appeared on the electrometer, as was evident by running through the procedure with $S6$ open so that the current was zero. A typical $I=0$ run is shown in curve d of Fig. 5. A rise averaging 3 mV appears during the first 2 seconds, followed by a smaller downward drift of long duration. In addition, an oscillating effect varying in magnitude from run to run from 0.5 to 2 mV was present.

None of these effects was correlated with I. They were easily subtracted from the current-correlated potential. The oscillations, whose magnitude varied from 6% to 20% of the magnitude of the I^2 effect were eliminated by smoothing. The initial rise and longer drift were accounted for by subtracting from the potential the average of eight $I=0$ runs which had been smoothed to eliminate oscillations.

Curves a–c of Fig. 5 show three runs with decaying current. To illustrate the procedure for correcting the signal the run shown in curve c of Fig. 5 was smoothed to eliminate the oscillations, after which the average of eight smoothed $I=0$ runs were subtracted to obtain curve e of Fig. 5.

The mean decay times for 11 runs are $\tau_I = 11.3 \pm 0.3$ sec and $\tau_\phi = 6.3 \pm 0.3$ sec. The mean value of the exponent n is 1.84 ± 0.09. The values of $\kappa\alpha$ ranged from 70 to 160.

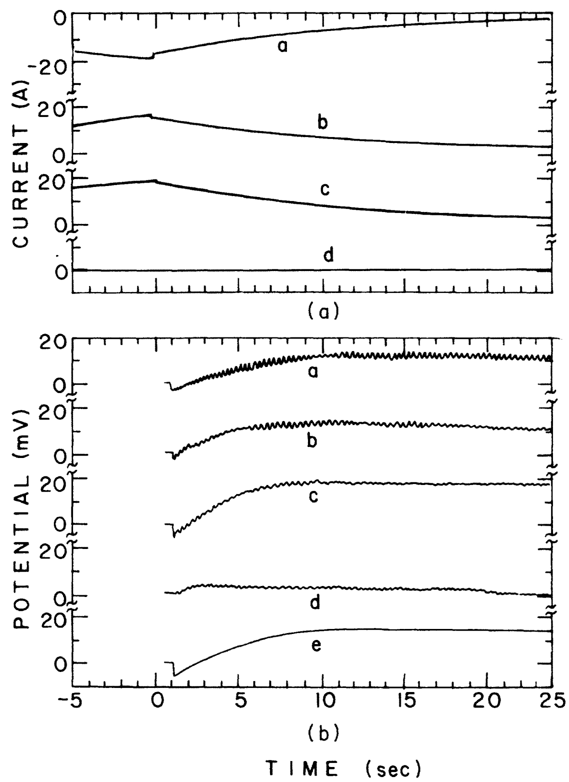

FIG. 5. Sample experimental data obtained in variation II, the Faraday-cage experiment. The "current" scale was inferred from magnetic-field readings. Except for curve e all of the potential curves are traced directly from the actual strip charts. Current curves c and d were also traced from the strip charts but there was a change of scale on a and b. A lapse of approximately one second can be noticed between the time the current began to decay and the beginning of electrometer measurement. The step in the current curves was due to magnetic fields resulting from currents in the feed-in lines which disappeared at time zero and therefore do not represent an actual current change in the coil. When the electrometer short, $S5$, is opened, a random contact potential of a few millivolts appears on the electrometer, explaining the immediate excursion of the potential from zero.

Of prime significance is the fact that the I^2 signal was still present. Since the currents are electrically isolated from the points between which the potential is measured, the effect appears to arise from a field or an action through a distance having a spacial dependence similar to that of electromagnetic fields and having as its source the currents in the wire. The signal appears to be a primary electromagnetic effect, as opposed to a secondary effect which depends upon contacts for transmission.

Specific implications from this experiment concerning other possible explanations will be discussed later.

C. Variation III

It has been questioned whether or not a function other than I^2 might better explain the observed effect. The present experiment was designed to help establish the functional nature of the signal.

A well-shielded persistent switch was reintroduced so that the current decay could be interrupted by putting the current into a persistent mode. By stopping the decay several times during a run the functional relationship could be tested.

Figure 4(d) shows the schematic diagram of the circuit. The values of L, R, and τ_I were the same as in variation II.

It was found that although the persistent switch did not cause a large baseline change as in the original experiment, the sudden introduction of heat caused a smaller potential to appear which was independent of the current. Even with $I=0$ a negative voltage would appear when the heat was applied. After about 2 sec this signal would plateau at approximately 3 mV and then remain constant as long as the heat was applied. When the heat was removed, the potential would go positive and slowly return to zero, taking approximately 80 sec.

It was found that in the range near the critical temperature this potential was independent of the heater current and, thus, of the superconductor temperature. The portion of the superconductor within the persistent switch could therefore be raised above and below the critical temperature with no influence on the electrometer as long as the heat was not removed altogether. This allowed the opening and closing of the persistent switch without introducing any detectable error voltage.

Thirteen runs were made, decaying the current in steps. The number of steps in a run varied from 3 to 7. One run is shown in Fig. 6(a). Six runs had positive current and seven had negative current. The length of time the circuit was maintained in the persistent state during an interruption varied from 8 to 42 sec, with approximately 17 sec for the typical step.

A least-squares analysis of the data from the thirteen runs was made to determine the power-law exponent for each. The mean value of the exponent for the thirteen runs is 1.92 ± 0.14.

During the same day the stepping experiments were being performed five runs with uninterrupted decays were made. The potential had very large magnitudes; for one run it was 83 mV. The values

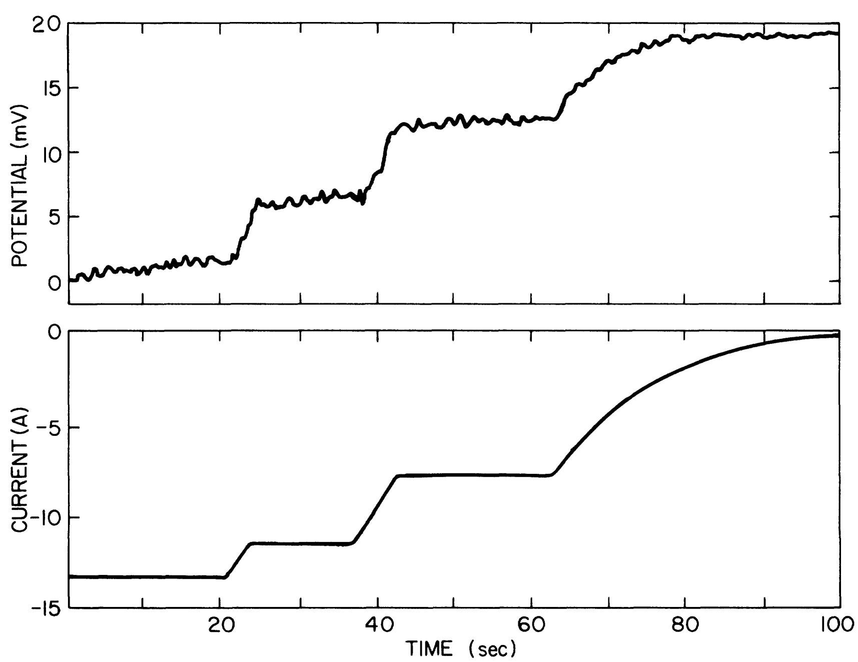

FIG. 6. An experimental run showing the potential ϕ and current I as functions of time in variations III. The curves have been drawn from information on the strip-chart recording of this run. The interruptions of the decay of I permit a distinction to be made between possible functions for ϕ as discussed in the text. The calculated value of n for this run is 1.94. Some electronic drift is evident.

of $\kappa\alpha$ range from 180 to 260. Figure 7 shows $I(t)$ and $\phi(t)$ from a sample of runs. The mean decay times were $\tau_I = 13.4 \pm 0.3$ sec and $\tau_\phi = 6.6 \pm 0.6$ sec. The inferred exponent is $n = 2.15 \pm 0.26$. These latter five runs provided additional information for use in evaluating thermoelectric error sources since the rate of production of heat in R had been changed.

D. Variation IV

This variation used the same circuit diagram as variation III but the apparatus was operated in helium II rather than helium I. Below the transition temperature, $T_\lambda = 2.17$ °K, the thermal properties of the liquid are vastly different from those above. The electrical conductivity remains at essentially zero but the effective thermal conductivity and heat capacity increase in such a fashion that heat transferred to helium II does not cause local boiling. Instead, it is immediately carried to the surface of the liquid, where a very thin film vaporizes. Thus, running in helium II entirely eliminates local boiling and removes any possibility of charge transfer on the bubbles.

In addition, because of its unusual thermal properties, helium II is an excellent heat sink. Because of this, the temperature rise of various components of the apparatus during a current decay is reduced.

In order to lower the bath temperature, the apparatus was modified to permit a reduction of the pressure over the liquid to at least 17 mm Hg, which corresponds to a temperature of 1.89 °K.

On one occasion, after clear signals had been observed when running with the helium above the λ point, six runs were made with the temperature between 1.93 °K and 2.01 °K. As inferred from the helium gas vapor pressure during the decay of the current, the temperature of the liquid remained constant within 0.001 °K.

The six runs were made with $S4$ open at all times to reduce noise. Four runs are shown in Fig. 8. The mean value of the decay constants are $\tau_I = 5.5 \pm 0.1$ sec and $\tau_\phi = 3.3 \pm 0.3$ sec, resulting in $n = 1.76 \pm 0.25$. The range of $\kappa\alpha$ was 18 to 32.

Several runs were also made from the persistent mode. Although they were not nearly as free of

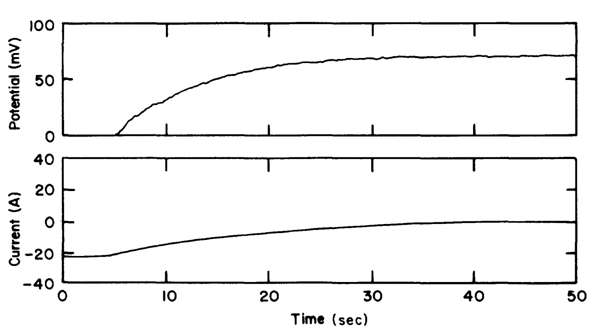

FIG. 7. An uninterrupted run in variation III. The magnitude of the potential, ϕ, is 74 mV. The figure has been traced from the actual strip-chart recording. At $t = 0$ the magnitude of the current is almost maximum and the electrometer input is grounded. At $t = 4.6$ sec the current source is removed and I begins to decay. At $t = 5.2$ sec the ground is removed from the electrometer input.

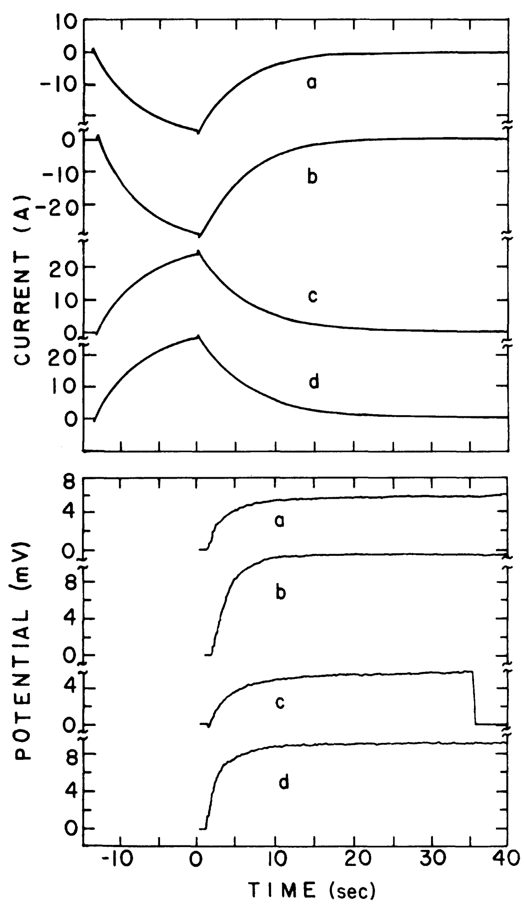

FIG. 8. Sample experimental data traced directly from the actual strip charts from variation IV, the experiment below the λ point. The current scale has been inferred from the magnetic field, which was the quantity actually recorded. The steps in the current curve were due to magnetic fields resulting from currents in the feed-in lines which disappeared at time zero and therefore do not represent an actual current change in the coil. The excursion, due to contact potentials, when the electrometer short, $S5$, is opened adds an uncertainty to the magnitude of the potential signal when the excursion occurs in the positive direction, as in runs ***a***, ***b***, and ***d***. On run *c* the electrometer was shorted at $t = 36$ sec. The values of $\kappa\alpha$ for the four runs are 18, 32, 23, and 32, respectively.

noise and systematic errors as the six discussed above, the I^2 signal was clearly distinguishable.

V. THE FUNCTIONAL NATURE OF THE EFFECT

The original experiment and the first two variations strongly suggested an I^2 function for the effect because ϕ is an even function of I and a fit to all the data results in an exponent near 2. Nevertheless, other functions should be considered.

Figure 9(a) illustrates how two different even functions of the current and its time derivatives can give much the same results. For instance, as long as $I(t)$ is exponential $(dI/dt)^2$ and I^2 have the same time-dependent nature. Except for a change in sign, the same is true of $I(dI/dt)$.

Figure 9(b) illustrates how an interruption of the decay of I will permit a clear distinction to be made between the functions being considered.

The primary purpose for variation III was to make this distinction. Figure 6 shows one of 13 experimental runs where the current decay was interrupted several times. These runs clearly eliminate all functions of I that we have considered except for I^2, which they support. Although there may exist a small admixture of functions dependent upon derivatives of the current the predominant function is I^2. The best fit of $\phi \propto I^n$ for the 13 runs gives $n = 1.92 \pm 0.14$.

The combined analysis of determinations of n from all experiments supports the interpretation of the signal as being dependent upon I^2. Table I gives the pertinent data. Weights were assigned to the data from each experiment after an examination of the strip charts for signal strength, noise, electronic drift, and other error sources. The best fit of $\phi \propto I^n$ to all the data results in the value $n = 2.02 \pm 0.05$.

In summary, the evidence from three categories very strongly favors the interpretation $\phi \propto I^2$ in agreement with Eq. (13). First, the signal is an even function of I. Second, $\phi \propto I^2$ is the only even function of I that we have found that agrees with the interrupted decay experiment in variation III. Third, the best fit of all the data from 49 runs results in the value $n = 2.02 \pm 0.05$.

VI. POSSIBLE SOURCES OF POTENTIALS

A. The self-Hall effect

The Hall-effect field depends upon $\vec{v} \times \vec{B}$, where $\vec{v}$ is the velocity of drifting charges and $\vec{B}$ is the magnetic field imposed upon a conductor. If the magnetic field is that produced by the conduction current itself, the resulting electric field will be dependent upon I^2.

Although the magnitude of the drift velocity in superconductors is much larger than in normal conductors carrying the same current, the potentials resulting from Hall-effect fields do not increase appreciably because, although the electric

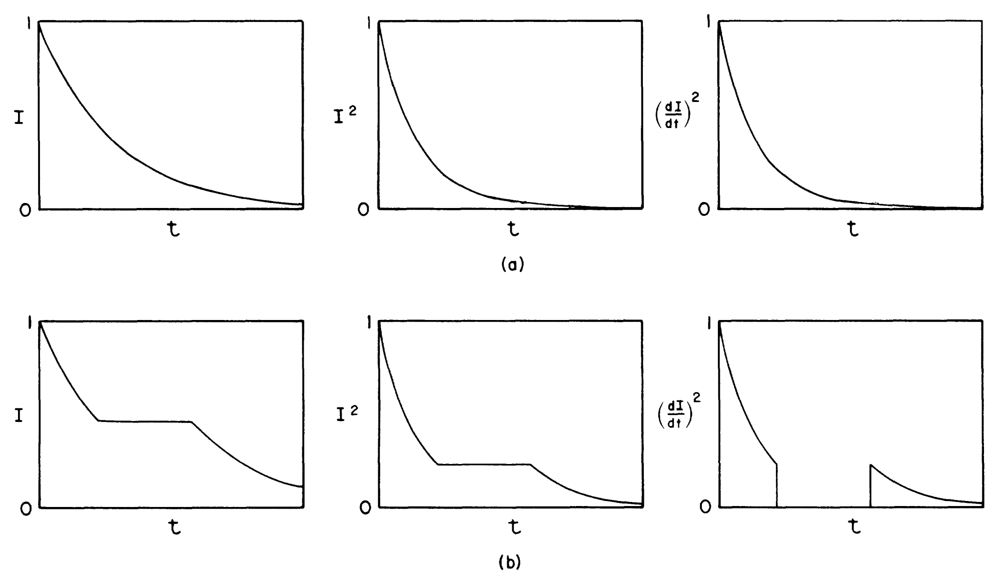

FIG. 9. When I is exponential, the functions I^2 and $(dI/dt)^2$ are the same within a constant multiplier, as illustrated in (a). When the exponential decay is interrupted, however, a clear distinction can be made between the two functions, as shown in (b). See Fig. 4 for comparison with the potential in an actual interrupted run. The observed potential appears to be proportional to $1-[I(t)/I_0]^2$.

TABLE I. Determinations of n resulting from a statistical fit of $\phi \propto I^n$ to the observed data.

Experiment	Current mode	Weight	Number of runs	Mean value of n
Original	Decaying	1	9	1.93 ± 0.13
Variation I	Decaying	2	5	2.70 ± 0.26
Variation II	Decaying	1	11	1.84 ± 0.09
Variation III	Decaying	3	5	2.15 ± 0.26
Variation III	Interrupted	2	13	1.92 ± 0.14
Variation IV	Decaying	2	6	1.76 ± 0.25
Results from all experiments			49	2.02 ± 0.05

fields increase greatly, the distances through which they act decrease proportionately.

Reed *et al.*, measured the Hall effect in superconducting niobium and indium.[24] Near 1 kG, which is the magnetic-field region pertinent to our experiment, their samples would act as type-II superconductors. In this field region they measured Hall-effect voltages on the order of 0.1 μV across a 0.4-mm-thick conductor.

Niessen and Staas have reported measurements of Hall-effect fields in type-II superconductors.[25] Samples 0.022 mm thick in a 1-kG external field developed potentials of approximately 30 μV.

(a) To estimate the Hall effect in our experiments we first consider the Hall potential resulting from the magnetic field inside the superconductor produced by the current in that same wire section. The $\vec{B}$ field may be thought of as having been produced by a long straight wire. For order-of-magnitude calculations we will adopt a naive model, imagining that the current density distribution in the wire varies as

$$j = \frac{I}{2\pi a \lambda} e^{-(a-r)/\lambda}, \tag{16}$$

where λ is the London penetration depth and r is the distance from the axis of the wire. The coefficient $I/2\pi a\lambda$ arises from $I = \int_0^a j dA$ for the case $\lambda \ll a$.

The magnetic field arising from this current density distribution would be

$$B = \frac{\mu_0 I}{2\pi a} e^{-(a-r)/\lambda}. \tag{17}$$

Now, since $\vec{v} = \vec{j}/\rho$ and $\vec{E} = \vec{v} \times \vec{B}$ we find

$$E = \frac{\mu_0 I^2}{4\pi^2 a^2 \rho \lambda} e^{-2(a-r)/\lambda}. \tag{18}$$

The electric potential developed between the center and outside a wire is obtained from $-\int_0^a E dr$ resulting in

$$\phi = \frac{\mu_0 I^2}{8\pi^2 a^2 \rho}. \tag{19}$$

The potential difference between the center and surface would be about 1.2×10^{-7} V for $I = 16$ A. Notice that the depth λ does not enter into the final expression for the voltage difference between the center and the outside of the wire. For calculations of upper limits the result can be applied to type-II superconductors and to nonsuperconducting portions of the circuit as well.

The effect of such a potential on our electrometer would be orders-of-magnitude smaller because, except for deviations from the assumed long-straight-wire formula, no electric field would be observed outside the wire. This is because at $r > a$ the wire appears charge neutral, with the interior having one sign and the surface another.

(b) In the second case we consider the Hall effect produced on a loop of wire by the magnetic field resulting from the inductive loops. This could charge the portion of a wire on the inside of the loop oppositely to that on the outside of the loop.

Again, the long-straight-wire formula may be used to calculate the $\vec{B}$ field acting on adjacent wires, so in this case $B = \mu_0 I/(2\pi r)$. For N inductive turns we may estimate $B_{max} < \mu_0 NI/2\pi a$. Using this expression for B instead of Eq. (17) we may calculate the maximum potential developed across the wire in a manner similar to the one preceeding, resulting in

$$\phi = \frac{\mu_0 I^2 N}{2\pi^2 a^2 \rho}. \tag{20}$$

This potential could be detected if a probe were properly positioned on the superconductor.

Actually, for all but variation II the electrometer input connects with the center of the brass shunt resistor. The Hall potential for that device would also depend upon $I^2 N$ but the magnitude would be much less because of its placement relative to the inductive loops. Equation (20) therefore represents an upper bound. Taking $I = 16$ A and $N = 19$ as in the original experiment, $\phi = 9 \times 10^{-6}$ V. This is a factor of 10^{-3} down from the observed signal. In Variation I, n was reduced to 4, a factor of 0.21 yet the signal *increased* a factor of 10. The Hall effect should have decreased. With $N = 4$ the magnitude of the Hall effect is 2×10^{-5} too low. In variations III and IV the placement of the shunt had been changed so a further check of the dependence on N could not be made.

In variation II voltages resulting from the self-Hall effect would be zero because the effect could only redistribute charges which would result in no field outside the Faraday cage. Nevertheless, the signal was still there.

For three reasons, then, the self–Hall effect is unable to explain the results: The possible self-Hall effect magnitudes are many orders of magnitude too small, the dependence on magnetic field is not borne out by experiment, and in the special Faraday-cage experiment no Hall potential would be expected, but the signal remained.

B. Configurational emf's

As reported by Chester, configurational emf's may arise in a circuit at points where the velocity of the charge carriers changes due to differences in geometry of material.[26] Thus, if a current divides at a junction, the drop in kinetic energy shows up as a reduced electric potential. This is analogous to the Bernoulli effect in fluids. It is dependent upon v^2 and in some of our variations would have the I^2 current relationship necessary to account for the signal if both pick-up points were, in effect, across the region where the change in v occurs.

In the present case an appreciable slowing arises where the superconductor meets the brass resistor, R. We will estimate the emf developed between the surface of the superconductor and the resistor, assuming that the speed of the charge carriers in the brass is zero. Using Eqs. (10) and (16) to estimate the drift speed on the surface of the superconductor we have

$$\phi = \frac{m}{e}\left(\frac{I}{2\pi a \lambda \rho}\right)^2 . \qquad (21)$$

For several reasons configurational emf's provide an attractive explanation for the effect. First, it has the I^2 dependence. Second, because it is basically a function of v^2 the expected potential would depend upon the current density distribution through the superconductor. In a type-II superconductor this distribution is nonunique which, through λ in Eq. (21), could account for the widely varying potential magnitudes we have observed. This is the only explanation considered here that has this property.

Unfortunately, there are two problems with the explanation. The first concern the signal magnitude. Taking $I = 16$ A and $\lambda = 10^{-3}\,a$ the potential becomes $\phi = 3 \times 10^{-8}$ V. For some of the runs in variation I this is a factor 2×10^{-7} smaller than the observed signal. To make up the deficit an unusually large increase in the estimates for the charge carrier velocity on the conductor surface would be required.

An even greater objection to this explanation arises from the results of the Faraday-cage experiment. The configurational emf can change the distribution of electrostatic charge in the circuit, thus leading to electric fields, but it cannot change the total charge. Since, classically, the total charge is the quantity responsible for a potential between the Faraday cage and ground, this effect cannot account for a signal in this case.

C. Nonsteady currents

In cases where a time-changing current exists, through the $\partial \vec{A}/\partial t$ terms in Maxwell's theory one might expect electric fields proportional to v_1^2 to show up. In the original experiment and in variations I, II, and IV there are two reasons why such fields might develop.

First, if the current is decaying, then even though at any given time the *present* current is the same everywhere in the coil, different portions of the coil would have different *retarded* currents, depending upon the position of the field point. In general, this would lead to electric fields.

This effect, however, is of higher order of smallness. It can be shown that in our experimental situation the fractional contribution to v^2/c^2 terms would be no greater than $4a/(\tau_I c) \approx 10^{-10}$. Since the possible potential arising from v^2/c^2 terms is already very small, this effect is completely negligible.

Second, a contribution might arise since the current in one portion of the coil would not be the same as in another because of time delay due to the finite signal velocity for current changes. This effect, however, is also higher order, the fractional contribution to v^2/c^2 terms being no greater than $(4\pi a N)/(\tau_I c) \approx 10^{-7}$. Again, this is completely negligible.

In variation III the currents are steady so even the tiny effects mentioned in the last two paragraphs would not be expected, and, therefore, this explanation can no longer be considered.

D. Thermoelectric effects

Several thermoelectric effects are possible mechanisms. The temperature changes that may lead to current-correlated effects result from I^2R joule heating in the shunt resistor R while the current is decaying.

Two approaches will be taken to the question. First, the general functional nature of the shunt temperature will be considered. Second, magnitudes of the temperature-dependent effects will be estimated.

The shunt material was brass. The values of R for the original experiment and variation I were, respectively, 82 and 118 $\mu\Omega$. For the last three variations $R = 64$ $\mu\Omega$. The temperature at any point in depends upon the geometry, the I^2R heat production, the specific heat of the material, and the losses to liquid helium and other materials.

If we assume no losses except to liquid helium and a uniform temperature through the resistor the differential equation for the temperature, T, above that of boiling liquid helium will be

$$cm\,\frac{dT}{dt} + dQ/dt = I_0^2 R e^{-2t/\tau_I}\ . \tag{22}$$

Here c is the heat capacity of brass, m is its mass, and dQ/dt is the rate of heat loss to helium. Dinaburg gives the heat loss from copper to boiling helium I in a graph[27] from which we infer the approximate function

$$dQ/dt = HAT^{3/2}\ , \tag{23}$$

where A is the effective area exposed to helium, and $H = 1.0$ W/(cm^2°K$^{3/2}$). Using a linear approximation to this function in the appropriate temperature region, Eq. (22) can be solved exactly. As is the case in the present experiments, when $2cm/\tau_I \ll HAT_{\max}{}^{1/2}$, where $T_{\max}$ is the maximum temperature above that of boiling helium, a particularly simple form for the solution results,

$$T = T_{\max}(e^{-t/\tau'} - e^{-2t/\tau_I})\ , \tag{24}$$

where

$$\tau' = cm/F\ ,\ F = [\tfrac{2}{3} I_0^2 R (HA)^2]^{1/3},\ \text{and}\ T_{\max} = I_0^2 R/F.$$

In the case of variation IV the limitation on dQ/dt is a thermal resistance between the brass resistor and the helium II bath. Wilks gives a graph[28] of this resistance, which for our bath temperature is 3.4 °K cm^2/W. From this we can readily find a value for F since the function dQ/dt is, in this case, already linear for small temperature differences.

Figure 10 shows an example of the application of Eq. (24). At $t = 0$ the temperature of R rises to a maximum within a time on the order of milliseconds. On the other hand, the observed electrometer signal ϕ makes no such immediate excursion. After reaching a maximum, T decays to zero while the observed signal builds up to a maximum. From this, it is clear that the signal is not proportional to the temperature of the resistor and any explanation requiring such a potential fails. With the exception of bubble nucleation all of the thermoelectric effects discussed below depend directly upon the temperature of R. Although such explanations are already ruled out because of the time-variation incompatibility it will be shown that the effect magnitudes, being many orders of magnitude too low, eliminate these mechanisms as well.

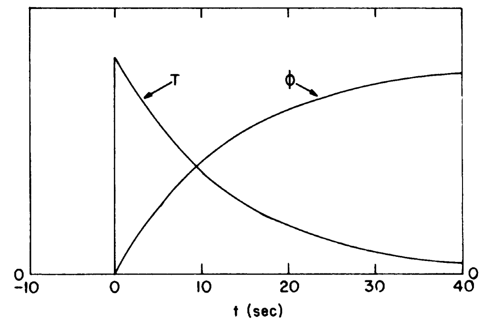

FIG. 10. The calculated shunt-resistor helium-bath-temperature difference, T, is shown as a function of time for an $I = 16$ A continuous run in variation III. A typical electrometer potential, ϕ, is shown for comparison. The temperature has a fast rise time on the order of a few milliseconds. Any potential effect which increases with temperature cannot explain the observed potential since the temperature difference would rise rapidly and then return to zero, whereas the potential rises more slowly from zero and retains its positive value.

To obtain estimates of the magnitudes of specific thermoelectric effects the maximum temperature differences arising in the apparatus in each variation have been estimated. The values obtained for the surface of the shunt resistor are given in Table II for a current of 16 A. The surface to interior temperature differences in R are estimated to be smaller. Temperature changes in other parts of the apparatus due to conduction of the heat produced in the shunt are also smaller in every case.

Seebeck effect. Thermocouple potentials could arise between the two superconductor-to-brass junctions on either side of R due to uneven heating in R. They could also arise in some variations between the signal junction and ground. The appropriate thermocouple coefficients[29] are expected to be less than 5 μV/°K, giving the potentials in Table II. In every case these are too low to explain the effect. In particular, the Seebeck effect would predict zero voltage in the Faraday-cage experiment since it would only redistribute charge on the circuit rather than change its total value.

Chemical potentials. As reported by deWaele

TABLE II. Upper limits of thermoelectric potentials arising from current-correlated temperature differences with values standardized to a current of 16 A.

Experiment	Maximum shunt to helim temperature difference (10^{-3} °K)	Electrometer potential (μV) Seebeck effect	Chemical potential	Helium desorption	Observed
Original	260	< 1.3	< 3	< 800	12000
Variation I	140	< 0.7	< 2	< 450	115000
Variation II	37	0	0	< 110	22000
Variation III (decaying)	37	< 0.2	< 0.4	< 110	41000
Variation IV	32	< 0.2	< 0.4	< 100	5000

et al., a change in the chemical potential of the conduction electrons would result in a voltage difference that would be temperature dependent.[30] They obtained values in the 10 μV/°K region for niobium samples. Again, as shown in Table II, the temperature differences give potential values that are much too small. The chemical-potential effect should be zero in variation II because it would not result in a total charge difference within the Faraday cage.

Helium desorption. A suggestion has been made that the effect arises from helium desorption from copper or perhaps some other material which changes temperature during a run. deWaele *et al.*, measured potential changes up to 3 mV/°K resulting from such a desorption from copper.[30] Both the present and the former apparatus were operated immersed in liquid helium, which would seem to eliminate such a possibility. In any event the temperature change is too small to account for the effect by this means, as shown in Table II.

Bubble nucleation. A suggestion has been made that a charge transfer might be occuring due to the boiling of helium resulting from joule heating in R. A negative-charge carrier would have a lower energy in helium vapor while a positive-charge carrier would have lower energy in the liquid. Thus, if a negative charge were somehow produced near the source of heat, it would be swept along with the bubbles as they rise in the liquid.

If such an effect were present, it would, indeed, explain the time dependence of the signal in the original experiment and in the first three variations. The mechanism might not account for the changes in signal magnitude as represented by different values of $\kappa\alpha$ although one could not affirm or deny this with confidence until a mechanism for charging the bubbles was identified.

Variation IV tests this explanation. After observing the signal in helium I the temperature was reduced to 1.95 °K which is below the λ point (2.17 °K). In helium II where no bubbles are formed, the signal was once again observed (see Fig. 8) with approximately the same magnitude as it had in helium I. For this reason bubble nucleation does not explain the effect.

It appears that no thermoelectric effect can account for the signal. The magnitudes are too low and the time variation of potentials arising from such effects is wrong.

E. Flux-motion potentials

In type-II superconductors electric fields are present due to the motion of flux-bearing supercurrent vortices. Usually these vortices are pinned but under certain conditions they may either creep or jump. In either case, the motion produces emf's.

In the critical state, where the magnetic forces balance the pinning forces, flux motion may occur due to thermal, electrical, or mechanical disturbance. The rapid vortex motion produces an emf.[31] Kim *et al.* have measured fields on the order of μV/mm.[32,33] These fields, however, are in the direction of the conduction current and therefore reverse when I is reversed. Furthermore, the resulting emf's show random jumps rather than a smooth behavior. For the above two reasons in addition to the fact that in all of the present experiments the fields were below the critical value, flux-motion emf's cannot explain the signal.

Flux creep due to thermally activated flux flow may occur below the critical field,[33,34] but this is an extremely small effect as verified by Kim *et al.*[32] and the fields are also in the direction of the transport current.

Because of the random behavior, magnitudes, and reversal with I flux flow emf's cannot explain the effect.

VII. CONCLUSIONS

None of the proposed explanations are in reasonable agreement with the observed signal in *any* of the experimental variations. For every experimental variation the magnitudes of every proposed effect is too low. In addition, the functional relationships with current and other parameters are wrong in most cases. Furthermore, for every proposed explanation there is at least one experimental variation which, taken alone, is decisive in eliminating it as a possibility.

To eliminate most explanations the Faraday-cage experiment, variation II, itself appears to be sufficient. For the following effects, the expected signal in this case would be zero: the self-Hall effect, configurational emf's, the Seebeck effect, chemical potentials, and flux-motion emf's. Nonsteady current effects are eliminated quite as surely by variation III. Charge transfer in boiling helium is eliminated by variation IV.

The intent of the experiments has been to check Maxwell's equations for I^2 electric-field effects in the experimental situation where the circuit is at rest and the charge-carrier speed is constant. The expected field is zero. Yet, the results of all experiments indicates a nonzero field with an I^2 dependence. The best fit of all the data by $\phi \propto I^n$ gives $n = 2.02 \pm 0.05$. No other function appears to agree with the observations.

ACKNOWLEDGMENTS

We appreciate the contributions of the Electrodynamics Laboratory, the Department of Electrical Engineering (USU), Russell M. Holdredge, and Eastman N. Hatch. The ideas, suggestions, and criticisms of John J. Merrill and V. Gordon Lind are gratefully acknowledged. We also acknowledge helpful discussions with D. A. Baker, W. A. Steyart, and others at Los Alamos Scientific Laboratory. The continued support and encouragement of USU Vice President Dean F. Peterson have been indispensable and are deeply appreciated.

---

*Work supported by Utah State University Vice President for Research.

[1]W. Farrell Edwards, *Measurement of an Electric Field Due to Conduction Currents* (Utah State Univ. Press, Logan, Utah, 1974).

[2]W. F. Edwards, Bull. Am. Phys. Soc. 20, 630 (1975).

[3]Sir Edmund Whittaker, *A History of the Theories of Aether and Electricity* (Harper, New York, 1960), Vol. I, pp. 201, 202.

[4]Alfred O'Rahilly, *Electromagnetics: A Discussion of Fundamentals* (Longmans, Green, and Co., London, 1938), pp. 523–535.

[5]Sir Edmund Whittaker, *A History of the Theories of Aether and Electricity* (Ref. 3), pp. 201, 202, 205.

[6]Alfred O'Rahilly, *Electromagnetics: A Discussion of Fundamentals* (Ref. 4), p. 525.

[7]J. C. Maxwell, quoted by Alfred O'Rahilly, *Electromagnetics: A Discussion of Fundamentals* (Ref. 4), p. 514.

[8]Sir Edmund Whittaker, *A History of the Theories of Aether and Electricity* (Ref. 3), p. 290.

[9]Sir Edmund Whittaker, *A History of the Theories of Aether and Electricity* (Ref. 3), p. 206.

[10]Alfred O'Rahilly, *Electromagnetics: A Discussion of Fundamentals* (Ref. 4), p. 589.

[11]Sir Edmund Whittaker, *A History of the Theories of Aether and Electricity* (Ref. 3), pp. 235–236.

[12]E. Klein, Z. Phys. 77, 417 (1932). The translation quoted appears in Alfred O'Rahilly, *Electromagnetics: A Discussion of Fundamentals* (Ref. 4), p. 589.

[13]D. A. Baker, Am. J. Phys. 32, 153 (1964). For a further discussion of this point see W. G. V. Rosser, *Classical Electromagnetism via Relativity* (Plenum, New York, 1968), pp. 272–284.

[14]A detailed consideration of properties of electric fields such as in Eq. (8) will appear in another publication. This will include the conditions limiting γ_1, γ_2, and γ_3 as a result of conservation of energy and other theorems.

[15]J. Bardeen and J. Stephen, Phys. Rev. 140, A1197 (1965).

[16]P. W. Anderson and Y. B. Kim, Rev. Mod. Phys. 36, 39 (1964).

[17]Y. B. Kim, C. F. Hempstead, and A. R. Strnad, Rev. Mod. Phys. 36, 43 (1964).

[18]J. E. Evetts, A. M. Campbell, and D. Dew-Hughes, Philos. Mag. 10, 339 (1964).

[19]Y. B. Kim, C. F. Hempstead, and A. R. Strnad, Phys. Rev. 129, 528 (1963).

[20]M. A. R. LeBlanc, Phys. Rev. 124, 1423 (1961).

[21]S. L. Wipf and M. S. Lubell, Phys. Lett. 16, 103 (1965).

[22]M. R. Beasley, W. A. Fietz, R. W. Rollins, J. Silcox and W. W. Webb, Phys. Rev. 137, A1205 (1965).

[23]Since the confidence interval corresponding to the standard deviation of a mean of n values varies when n is small we have chosen to report uncertainties which represent 70% confidence intervals computed from the t distribution. These reflect the scatter of the data about the mean. The uncertainties have not been increased to allow for unknown systematic errors.

[24]S. A. Reed, E. Fawcett, and Y. B. Kim, Phys. Rev. Lett. 14, 790 (1965).

[25]A. K. Niessen and F. A. Staas, Phys. Lett. 15, 26 (1965).

[26]M. Chester, Phys. Rev. Lett. 5, 91 (1960).

[27]L. B. Dinaburg, Cryogenics 11, 239 (1971).

[28]J. Wilks, *The Properties of Liquid and Solid Helium* (Clarendon, Oxford, 1967), p. 424.

[29]R. Berman, in *Advanced Cryogenics,* edited by C. A. Bailey (Plenum, London, 1971), p. 130.

[30]A. Th. A. M. deWaele *et al.*, Physica 65, 587 (1973).

[31]C. P. Bean, Phys. Rev. Lett. 8, 250 (1962).

[32]Y. B. Kim, C. F. Hempstead, and A. R. Strnad, Phys. Rev. Lett. 9, 306 (1962).

[33]Y. B. Kim, C. F. Hempstead, and A. R. Strnad, Phys. Rev. 139, A1163 (1965).

[34]P. W. Anderson, Phys. Rev. Lett. 9, 309 (1962).